



Motion fading is driven by perceived, not actual angular velocity

P.J. Kohler^{a,*}, G.P. Caplovitz^{a,b,c}, P.-J. Hsieh^a, J. Sun^a, P.U. Tse^a

^a Department of Psychological and Brain Sciences, Moore Hall, Dartmouth College, Hanover, NH, USA

^b Princeton Neuroscience Institute, Princeton University, Princeton, NJ, USA

^c Department of Psychology, Princeton University, Princeton, NJ, USA

ARTICLE INFO

Article history:

Received 10 January 2010

Received in revised form 25 March 2010

Keywords:

Motion

Form

Motion fading

Form–motion interactions

ABSTRACT

After prolonged viewing of a slowly drifting or rotating pattern under strict fixation, the pattern appears to slow down and then momentarily stop. Here we examine the relationship between such 'motion fading' and perceived angular velocity. Using several different dot patterns that generate emergent virtual contours, we demonstrate that whenever there is a difference in the perceived angular velocity of two patterns of dots that are in fact rotating at the same angular velocity, there is also a difference in the time to undergo motion fading for those two patterns. Conversely, whenever two patterns show no difference in perceived angular velocity, even if in fact rotating at different angular velocities, we find no difference in the time to undergo motion fading. Thus, motion fading is driven by the perceived rather than actual angular velocity of a rotating stimulus.

© 2010 Elsevier Ltd. All rights reserved.

1. Introduction

After prolonged viewing of a slowly drifting or rotating pattern under strict visual fixation, the pattern appears to slow down and then momentarily stop, even though the stationary form of the pattern remains visible. This illusory stopping or 'motion fading' has been reported to occur over rotating gratings and spinning sector disks (Campbell & Maffei, 1979, 1981; Cohen, 1965; Hunzelmann & Spillmann, 1984; Lichtenstein, 1963; MacKay, 1982), as well as stimuli comprised of dots (Hsieh & Tse, 2007, 2009a, 2009b). Several factors, including retinal eccentricity, number of sectors, dot organization, and angular velocity, have been shown to affect the time required for motion fading (Hsieh & Tse, 2007, 2009a, 2009b; Hunzelmann & Spillmann, 1984).

We have recently demonstrated that the spatial arrangement of otherwise identical orbiting dots can affect the time it takes to undergo motion fading (Hsieh & Tse, 2007). In particular, the time it takes for a set of dots rotating around a virtual center to be perceived as stopped (although in fact still continually moving) increases significantly when the dots can be grouped into the shape of a cross relative to when they cannot, even when all dot motions, in a local sense, are identical between the two conditions. This suggests that motion fading must occur at or after a stage

where global motion signals have been computed on the basis of local motion signals. One reason why the time needed to undergo motion fading varies with configuration may be that, once grouped, the set of moving dots generates 'emergent motion signals'. These motion signals are 'emergent' because they are not present in the image, but instead arise from virtual contours and contour features that exist after grouping operations have linked the dots into virtual continuous contours that themselves move as the dots move (Caplovitz & Tse, 2007; Kohler, Caplovitz, & Tse, 2009). The emergent component motion signals arising from the virtual arms of a cross configuration of dots is greater than the motion signals arising from the non-cross configuration. Motion fading presumably takes longer in the case of the cross configuration because as the strength of such emergent motion signals increases, the magnitude of represented motion vectors that must adapt to zero in order for motion fading to occur also increases (Hsieh & Tse, 2007).

We have also shown that the spatial configuration of dots can influence the perceived angular velocity at which they are perceived to rotate. Specifically, we have shown that, as is the case for continuous contours (Caplovitz, Hsieh, & Tse, 2006), dots arranged to form a virtual thin, high aspect ratio ellipse will appear to rotate faster than those that form a lower aspect ratio ellipse even when the two in fact rotate at the same angular velocity (Caplovitz & Tse, 2007). This observation raises the important question of whether the effect of spatial configuration on motion fading arises from the mere presence of emergent motion signals, or whether it arises from the perceived angular velocity as determined by the emergent motion signals. In particular, does motion

* Corresponding author. Fax: +1 603 646 1419.

E-mail addresses: peter.kohler@dartmouth.edu (P.J. Kohler), gcaplovi@princeton.edu (G.P. Caplovitz), pjh@mit.edu (P.-J. Hsieh), jie.sun@dartmouth.edu (J. Sun), peter.u.tse@dartmouth.edu (P.U. Tse).

fading take longer for the cross configuration because it appears to rotate faster than the non-cross configuration?

Here we answer this question by measuring motion fading and perceived angular velocity of various dot-configuration stimuli. If motion fading is driven by perceived angular velocity, we would expect to find differences in the duration needed to undergo motion fading whenever there is a difference in perceived angular velocity, even if there is no difference in actual angular velocity. Conversely, whenever the configurations show no differences in perceived angular velocity, we expect to find no difference in the time needed to undergo motion fading, even when actual angular velocities differ. However, if motion fading is not driven solely by the perceived angular velocity of the moving stimuli, but, in part, by the actual angular velocity, then two moving patterns may differ in the time needed to undergo motion fading even when they have the same perceived angular velocity.

2. Experiment 1. High aspect ratio rotating ellipses defined by closely spaced dots take longer to undergo motion fading than lower aspect ratio ellipses

A thin, high aspect ratio ellipse will appear to rotate faster than a fatter, low aspect ratio ellipse (Caplovitz et al., 2006). This is also the case if the elliptical contours are defined by small, closely spaced dots (Caplovitz & Tse, 2007). This is particularly intriguing because the speed at which each dot is locally moving is on average greater for a fat ellipse than for a skinny ellipse, because dots comprising a fat ellipse are on average further from the center of rotation. However, when the dots are spaced too far apart, there is no effect of configuration on perceived angular velocity (Caplovitz & Tse, 2007). In Experiments 1a and 1b we measured the time it takes to undergo fading for rotating ellipses defined either by widely or closely spaced dots, with different aspect ratios, all rotat-

ing at the same slow angular velocity. Specifically, in each case we tested whether ‘thinner’ dotted ellipses require a longer time to stop (TTS) than ‘fatter’ ones. In all experiments dots were of identical luminance contrast in all conditions, to control for the potential influence of luminance contrast on perceived motion (Anstis, 2003; Stone & Thompson, 1992; Thompson, 1982; Thomason & Stone, 1997; Thompson, Stone & Swash, 1996).

2.1. Methods

2.1.1. Observers

Seven subjects (six naïve and one author) participated in both the ‘a’ and ‘b’ versions of this experiment. All subjects had normal or corrected-to-normal vision, and the naïve subjects were paid for their participation. Before each experiment, and all the following experiments, the subjects underwent several training trials until they were accustomed to the experimental procedure.

2.1.2. Stimuli and procedures

The stimulus configurations and experimental procedures in Experiments 1a and 1b were identical except that in Experiment 1a the contours of the ellipses were defined by 12 small (0.02° visual degrees in diameter) white (128 lumen/m^2) equally spaced dots presented on a black ($\sim 0 \text{ lumen/m}^2$) background (Fig. 1a), while in Experiment 1b, the contours of the ellipses were defined by 32 such dots (Fig. 1b).

In each trial, a single ellipse was positioned so that its center was located 11 visual degrees along the horizontal axis either to the left or right of the central fixation spot. The ellipse had an aspect ratio that was either ‘fat’: $25/15$ ($4.85^\circ \times 2.91^\circ$ visual angle) or ‘thin’: $25/6$ ($4.85^\circ \times 1.16^\circ$ visual angle). The ellipse would rotate about its center at an angular velocity of either 2.94 deg/s or, as a control, a stationary ellipse would be presented. We have previously shown, using much higher angular velocities than those used

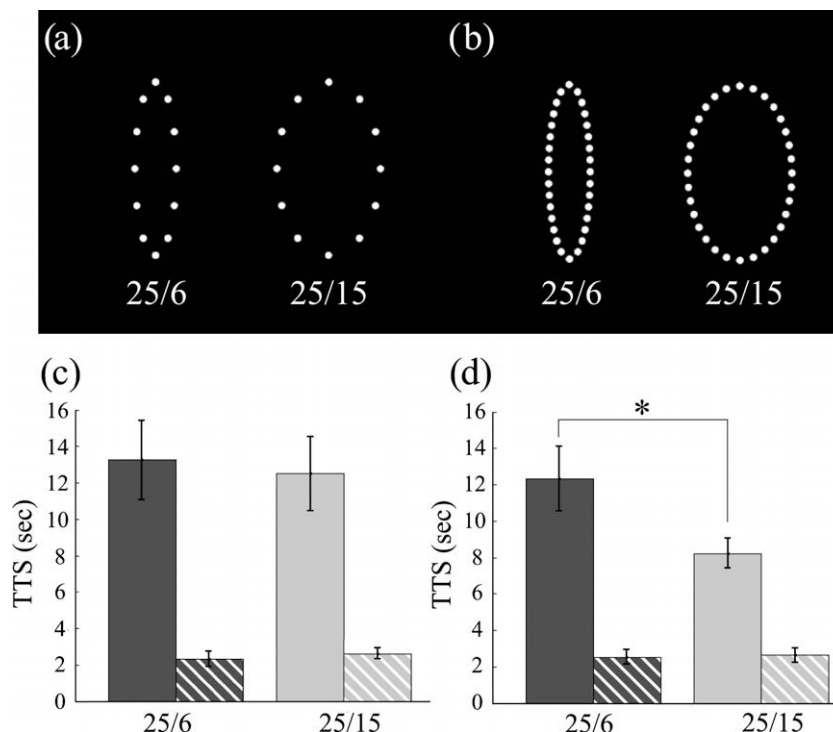


Fig. 1. Motion fading occurs faster for fatter than thinner dotted ellipses for the 32 dot case, but not for the 12 dot case. (a) The stimuli used in Experiment 1a, where ellipses were defined by 12 dots. (b) The stimuli used in Experiment 1b, where ellipses were defined by 32 dots. (c) The results of Experiment 1a. (d) The results of Experiment 1b. Solid bars indicate the time to stop (TTS) when the dotted ellipses were rotating. Striped bars indicate TTS when the ellipses were stationary. Error bars show the standard error of the mean.

to generate motion fading, that such fat and thin ellipses will appear to rotate at the same angular velocity in the 12 dot case, whereas in the 32 dot case the thin ellipse will appear to rotate faster than the fat ellipse (Caplovitz & Tse, 2007). The aspect ratio and angular velocity were pseudo-randomized across 20 trials per Experiment (1a and 1b), for each subject. The left or right position was interleaved across trials, so that a left trial would always be followed by a right trial, to avoid any possible after-image or other potential fatigue or adaptation effects across trials.

The direction of rotation was randomly determined for each trial. Subjects were required to press a button when the motion first appeared to fully stop. The control conditions in which the ellipse was in fact stationary provided a baseline reaction time for judgments of perceived stopping.

All the stimuli were viewed with both eyes in all experiments. The total size of the visual field was 40 cm × 30 cm, viewed from a distance of 57 cm. Subjects had their chin in a chin rest. The visual stimulator was a 2 GHz Dell workstation running Windows 2000. The stimuli were presented on a MITSUBISHI 2070SB CRT gamma-corrected monitor with 1280 × 1024 pixels resolution and 85 Hz frame rate. Eye movements were monitored using a head-mounted eye tracker (Eyelink2, SR research, Ontario, Canada). Trials during which the subject's monitored left eye was outside a fixation window of 1.5 visual degrees radius for more than 200 ms (to allow for eye blinks), were forced to abort. Trials recommenced when the subject regained fixation. Thus all data reported here were carried out under conditions of fixation.

2.1.3. Data analysis

A two-tailed paired *t*-test was performed in order to determine whether the time to apparent stopping was significantly different between the two tested aspect ratios.

2.2. Results and discussion

Results of Experiment 1a in which the ellipses were defined by 12 dots, are shown in Fig. 1c. The two striped bars show the reaction times when the stimuli were stationary. The filled bars show the results for the rotating ellipse. For both the moving [$t(6) = 0.329$, $p = 0.753$; mean $TTS_{high} = 13.25$ s, mean $TTS_{low} = 12.50$ s] and the stationary [$t(6) = 0.662$, $p = 0.532$; mean $TTS_{high} = 2.33$ s, mean $TTS_{low} = 2.61$ s] conditions, time to stop (TTS) does not differ between the two aspect ratios. Importantly the TTS is significantly longer when the stimuli were in fact moving as compared to when they were stationary; a repeated measures ANOVA revealed a significant main effect of angular velocity [$F(1, 6) = 34.07$, $p < 0.01$, measure of effect size $\eta^2 = 0.850$], but no significant effect of aspect ratio, and no significant interaction. This implies that subjects were able to initially perceive the stimuli as moving and accurately report their perception of motion fading.

Results of Experiment 1b are shown in Fig. 1d. Again, the striped bars show the reaction times when the stimuli were stationary. The dark grey and light grey filled bars show that TTS was significantly shorter for the low aspect ratio ellipse, when the stimulus was actually moving [$t(6) = 2.869$, $p < 0.05$; mean $TTS_{high} = 12.32$ s, mean $TTS_{low} = 8.23$ s], but not when it was stationary [$t(6) = 0.599$, $p = 0.571$; mean $TTS_{high} = 2.52$ s, mean $TTS_{low} = 2.63$ s].

The faster the perceived angular velocity, the longer it takes to undergo motion fading. These data are consistent with the previously reported finding that perceived angular velocity increases as aspect ratio increases for ellipses defined by closely spaced dots, as in the 32 dot condition, but not for widely spaced dots, as in the 12 dot condition. This suggests that motion fading is mediated by the perceived angular velocity of the moving stimuli rather than the magnitudes of the local motion signals that are measurable in the image (Caplovitz & Tse, 2007). It is interesting to note that

the TTS for the 32 dot thin ellipse is quite similar to the TTS for the 12 dot thin ellipse (and the 12 dot fat ellipse). This suggests that simply increasing the number of dots, while preserving the overall shape of the object does not influence the TTS. This is interesting because a simple model based on the adaptation of local motion signals might predict a longer TTS when more dots, and thus more sources of motion information, are present in the image. The fact that this is not the case further suggests that motion fading is mediated by emergent, rather than local sources of motion information (Caplovitz & Tse, 2007; Hsieh & Tse, 2007).

3. Experiment 2. Motion fading is fully accounted for by perceived angular velocity

Here we use a two-alternative-forced-choice (2AFC) paradigm to investigate the relationship between perceived angular velocity and TTS. In this pair of experiments we systematically vary the actual angular velocity, and measure the relative perceived angular velocity (Experiment 2a) and relative TTS (Experiment 2b) for high and low aspect ratio ellipses defined by 32 dots. This approach allows us to derive the angular velocities at which a fat and thin ellipse need to rotate in order to be perceived as rotating at the same angular velocity, and compare this to the angular velocities at which these same stimuli would need to rotate in order for motion fading to occur at the same time.

3.1. Methods

3.1.1. Observers

Eight subjects participated in Experiment 2a and a different group of eight subjects in Experiment 2b. All subjects were naïve, had normal or corrected-to-normal vision, and were paid for their participation.

3.1.2. Stimuli and procedures

In Experiment 2a, subjects were presented in each trial with two rotating ellipses defined by small white, equally spaced dots (32 dots) presented on a black background for 1000 ms (Fig. 2a). Each ellipse was positioned so that its center was located 11 visual degrees along the horizontal axis away from the central fixation spot. One ellipse (control) had the same aspect ratio = 25/15 (4.85° × 2.91° visual angle) and same angular velocity (4.2 deg/s) on every trial. The other ellipse (test) had an aspect ratio pseudo-randomly selected to be either 25/15 or 25/6 (4.85° × 1.16° visual angle). The test ellipse had an angular velocity pseudo-randomly selected on each trial from the following list: 0.42, 2.52, 3.36, 4.2, 5.04, 5.88, or 7.98 radial deg/s, so that for each angular velocity, 20 trials of each pairing were presented during an entire run (280 trials). Although both the control ellipse and test ellipse rotated in the same direction, the common direction of rotation was randomly determined for each trial. Subjects were required to indicate by pressing one of two buttons (2AFC) which of the two ellipses appeared to be rotating faster; the one to the left or the one to the right of fixation. In each trial, the control ellipse was randomly assigned to one side of the screen, and the test ellipse to the other.

In Experiment 2b, all procedures were identical to those in Experiment 2a except for the following differences. The test ellipse had an angular velocity pseudo-randomly selected on each trial from the following list: 0.84, 3.36, 4.2, 5.04, or 7.56 radial deg/s. Subjects were required to indicate by pressing one of two buttons (2AFC) which of the two ellipses appeared to stop first; the one to the left or the one to the right of fixation. The stimuli remained visible until a button was pressed. After a button was pressed, the screen turned black with only the fixation spot visible. Subjects were required to rest until the afterimage disappeared before they

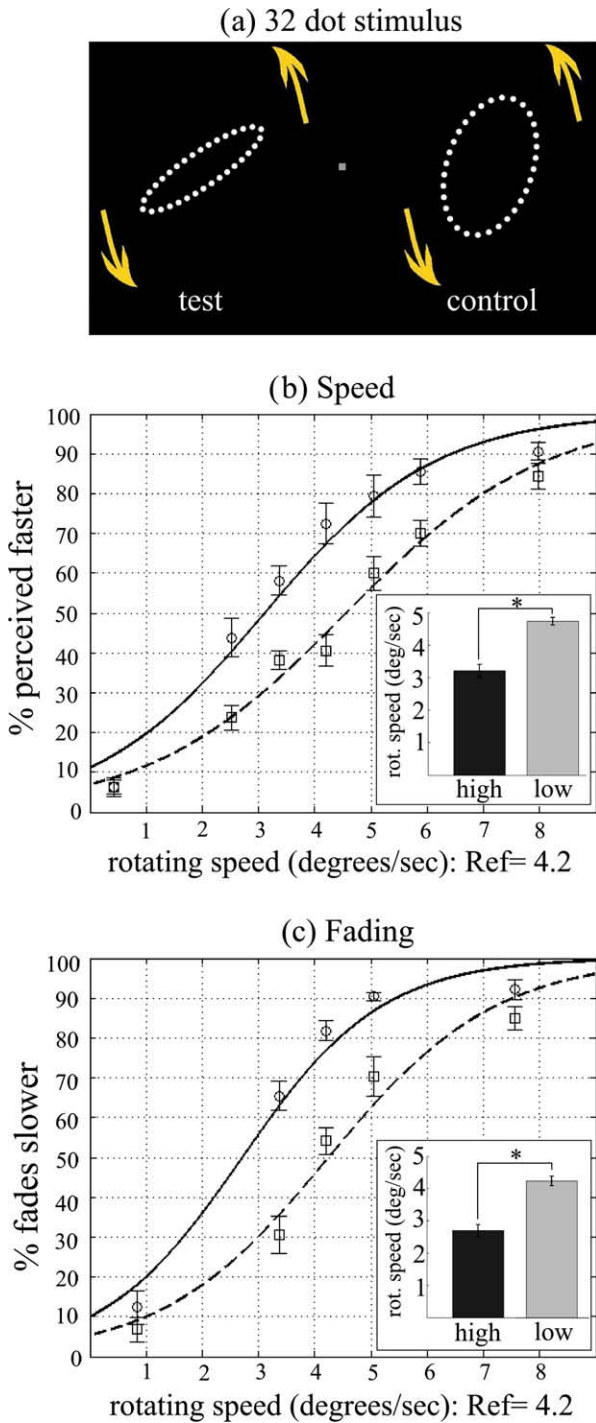


Fig. 2. Thin ellipses appear to rotate faster and fade slower than fat ellipses. (a) The stimuli used in Experiment 2. (b) The results of Experiment 2a. (c) The results of Experiment 2b. The mean of the psychometric response functions across subjects for high (solid line with round datapoints) and low (dashed line with square datapoints) aspect ratio test ellipses, is plotted on the two main graphs. The insets show the mean of the PSEs for the high (dark grey) and low (light grey) aspect ratio test ellipses.

started the next trial. For each angular velocity, 10 trials of each pairing were presented during an entire run (100 trials). For one subject, 24 trials of each pairing were presented, with a total of 240 trials. This was done to verify the effects with a larger number of trials. All data reported here were carried out under conditions of fixation, with eye movements monitored in the same way as described for Experiment 1, with the same fixation criteria.

3.1.3. Data analysis

In Experiment 2a, the percentage of trials that each test ellipse was perceived to rotate faster than the control ellipse was computed independently for each subject. Responses in Experiment 2b associated with outlier reaction times were removed from the analysis using a quartile approach. Reaction times more than 1.5 times the interquartile range below the first quartile, or above the third quartile, were considered to be outliers. In addition, responses with reaction times that were below 400 ms were removed, based on the assumption that this is the minimum amount of time required to make this kind of perceptual judgment. These criteria were used to remove outliers for all the 2AFC fading experiments reported in this paper. In Experiment 2b, we excluded an average of 4.75 responses per subject (maximum responses excluded for a single subject was 10).

We computed the percentage of trials in which the test ellipse appeared to undergo motion fading first. Thus in both experiments, for each of the two test ellipses, a value was calculated for each angular velocity. The following function was then fit to the corresponding data for each aspect ratio using MATLAB: $f(x) = 100 \times \left[\frac{e^{b_1+xb_2}}{1+e^{b_1+xb_2}} \right]$. The means of the resulting curves across subjects are plotted in Fig. 2b and c. For statistical purposes, the point of subjective equality (PSE, $x = -b_1/b_2$ i.e. the angular velocity at which each test ellipse needs to rotate in order to be perceived as rotating at the same angular velocity as the control ellipse) was computed for each subject. These values were determined by interpolating the 50% chance level from the logit functions fit to the data. Two-tailed paired *t*-tests were used to compare the PSEs of the thin and fat aspect ratio ellipses in both Experiments 2a and 2b. A two-tailed, independent samples *t*-test was used to compare the PSEs derived for perceived angular velocity in Experiment 2a with the PSEs derived for TTS in Experiment 2b. If the difference in TTS during motion fading is primarily mediated by differences in perceived angular velocity, we would expect the derived PSEs to be indistinguishable from each other.

3.2. Results and discussion

Fig. 2b illustrates the psychometric data and derived points of subjective equality for the two aspect ratios in Experiment 2a. Fig. 2c illustrates the results of Experiment 2b. The sigmoidal shape of the curves in Fig. 2c indicate that in general the faster a stimulus rotates, the longer motion fading takes to occur. Paired samples *t*-tests revealed that both for the angular velocity [$t(7) = 5.640, p < 0.001$] and the TTS [$t(7) = 10.584, p < 0.001$], the PSE for the thin ellipse was lower than for the fat ellipse. This indicates that in order to be perceived as rotating at the same angular velocity or in order for motion fading to occur at the same time, the skinny ellipse had to rotate slower than the fat ellipse. Importantly, a direct comparison of the two derived PSEs for the thin ellipses, using an independent samples *t*-test, showed no significant difference between them [$t(14) = 0.027, p = 0.979$]. This indicates that if the angular velocity of the thin ellipse had been adjusted so it appeared to rotate at the same angular velocity as the fat ellipse, then motion fading would occur at the same time for both aspect ratios. We can conclude that the differences in TTS during motion fading observed in Experiment 1 can be accounted for by differences in perceived angular velocity.

4. Experiment 3. Virtual contour differences can affect perceived angular velocity and TTS during motion fading

Although the results of Experiments 1 and 2 suggest that TTS during motion fading is primarily driven by the perceived angular velocity of the moving stimuli, it could be that this is only the case

for the specific elliptical dot configurations that we used for those experiments. In order to make more general conclusions about differences in motion fading, it is useful to test whether the results that we found in Experiments 1 and 2 can be replicated using other dot configurations. To that end, we here use two alternative dot configurations, in the shape of a square and a cross. If the results above can be generalized beyond the specific elliptical dot configurations used, we would expect to find the same result for these new configurations, namely that whenever there is a difference in perceived angular velocity there is also a difference in TTS, and when there is not, there is no difference in TTS.

4.1. Methods

4.1.1. Observers

Sixteen subjects carried out Experiment 3.1, with eight being subjects in 3.1a and another eight in 3.1b. Twelve subjects carried out Experiment 3.2, with six being subjects in 3.2a, and another six in 3.2b. All subjects were naïve, had normal or corrected-to-normal vision, and were paid for their participation.

4.1.2. Stimuli and procedures

The stimulus configuration in Experiment 3 is shown in Fig. 3a–c. There were two sub-experiments, and each one of them had two conditions (conditions a and b). In each sub-experiment, the only difference between the two stimuli was in how they could be non-locally perceptually grouped; they were identical at the level of local dot motions.

In Experiments 3.1a and 3.1b, subjects were presented on each trial with two rotating stimuli defined by 32 small grey (11.1 lumen/m²) dots (0.15° in diameter) presented on a black background (Fig. 3a). The dots were arranged to form either a cross or square. The 32 dots in the cross configuration were arranged as if there were four arms, each having eight dots centered 0.72°, 0.95°, 1.18°, 1.42°, 1.66°, 1.85°, 2.07° and 2.35° away from the center of

the cross. The 32 dots in the square configuration were arranged to form a square with dimensions $3.3^\circ \times 3.3^\circ$ visual angle, such that the lengths of the diagonals matched the dimensions of the cross configuration. The dots were equally spaced around the square contour. On every trial, the two stimuli were positioned on opposite sides of fixation so that their centers were located 11.3 visual degrees along the horizontal axis away from the central fixation spot, and 7.5 visual degrees above or below the central fixation spot. Upper and lower positions were interleaved, so that an ‘above’ trial would always be followed by a ‘below’ trial, to avoid any possible after-image or other potential confounding effects due to adaptation across trials. One stimulus (control) was always a square and had the same angular velocity (7.56 deg/s) on every trial. The other (test) stimulus was either the same square or a cross.

In Experiment 3.1a, on each trial the two stimuli were presented for 1000 ms and the test stimulus had an angular velocity pseudo-randomly selected on each trial from the following list: 3.36, 5.88, 6.72, 7.56, 8.40, 9.24, 11.76 deg/s, so that for each angular velocity, 20 trials of each pairing were presented during an entire run (280 trials). Although both the control and test stimulus rotated in the same direction, the common direction of rotation was randomly determined for each trial. Subjects were required to indicate by pressing one of two buttons (2AFC) which of the two stimuli was rotating faster; the one to the left or the one to the right of fixation. In each trial, the control stimulus was randomly assigned to one side of the screen, and the test stimulus to the other. Once again, all data reported were collected under conditions of fixation, with eye movements being monitored in the same way as described for the first two experiments, and with the same fixation criteria.

In Experiment 3.1b, all procedures were identical to those in Experiment 3.1a except that the stimuli remained visible until the subjects pressed a button. Subjects were required to indicate by pressing one of two buttons (2AFC) which of the two ellipses

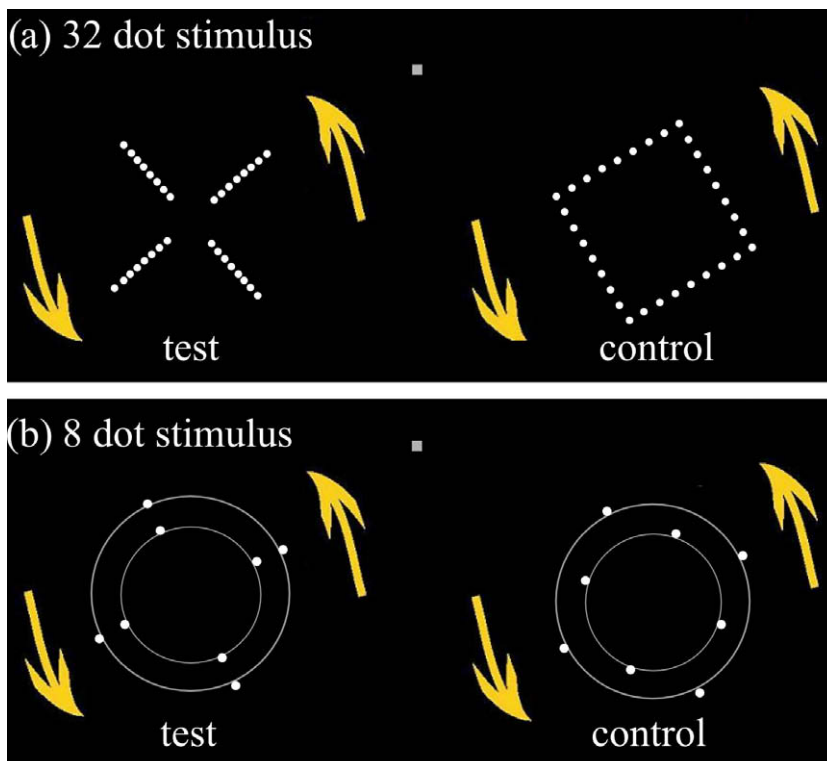


Fig. 3. Stimuli presented in Experiment 3, as they would appear in the bottom half of the screen. (a) The stimulus configuration for Experiment 3.1. (b) The stimulus configuration for Experiment 3.2. Note that the circles shown in (b) did not appear in the actual experiments.

appeared to stop first; the one to the left or the one to the right of fixation. In addition, the test stimulus in Experiment 3.1b had an angular velocity pseudo-randomly selected on each trial from the following list: 4.2, 6.27, 7.56, 8.4, or 10.92 deg/s, so that for each angular velocity, 10 trials of each pairing were presented during an entire run (100 trials).

In Experiments 3.2a and 3.2b, all procedures were identical to those in Experiments 3.1a and 3.1b, respectively, except that subjects were presented on each trial with two rotating stimuli defined by 8 dots rather than 32. (Fig. 3b). The 8 dots in the cross stimulus were arranged as if there were four arms, each having 2 dots centered 1.66°, and 2.35° away from the center of the cross. The dots in the square configuration were equally spaced and positioned so the dimensions were 3.3° × 3.3°, again matching the dimensions of the cross configuration.

4.1.3. Data analysis

The percentage of trials that the test stimulus was perceived to rotate faster (3.1a, 3.2a) or stop sooner (3.1b, 3.2b) than the control stimulus was computed, and the points of subjective equality were computed as described above for Experiment 2. We used the same outlier removal approach as described above, and excluded an

average of 0.75 (for Experiment 3.1b) and 2 (for Experiment 3.2b) responses per subject (maximum responses excluded for a single subject was 2 for 3.1b and 6 for 3.2b). Two-tailed paired *t*-tests were performed on the derived PSEs for the cross and square stimuli, to test if dot configuration led to differences in perceived angular velocity (3.1a, 3.2a) and TTS (3.1b, 3.2b). Two-tailed independent samples *t*-tests were used to compare the PSEs derived for perceived angular velocity with those derived for TTS in the 32 dot (3.1a, 3.1b) and 12 dot (3.2a, 3.2b) experiments.

These analyses allowed us to determine if, as was the case for elliptical contours, differences in TTS arising from dot configuration can be accounted for by differences in perceived angular velocity. If this is the case, then whenever there is a difference between the perceived angular velocities of the two stimuli, there should be a corresponding difference in the TTS.

4.2. Results and discussion

The result of Experiment 3.1a shows that, when the stimuli were defined by 32 dots as shown in Fig. 3a, the mean of the PSEs of the cross stimulus was significantly smaller than the mean of the PSEs of the square stimulus [$t(7) = 2.953$, $p < 0.05$] (Fig. 4a), mean-

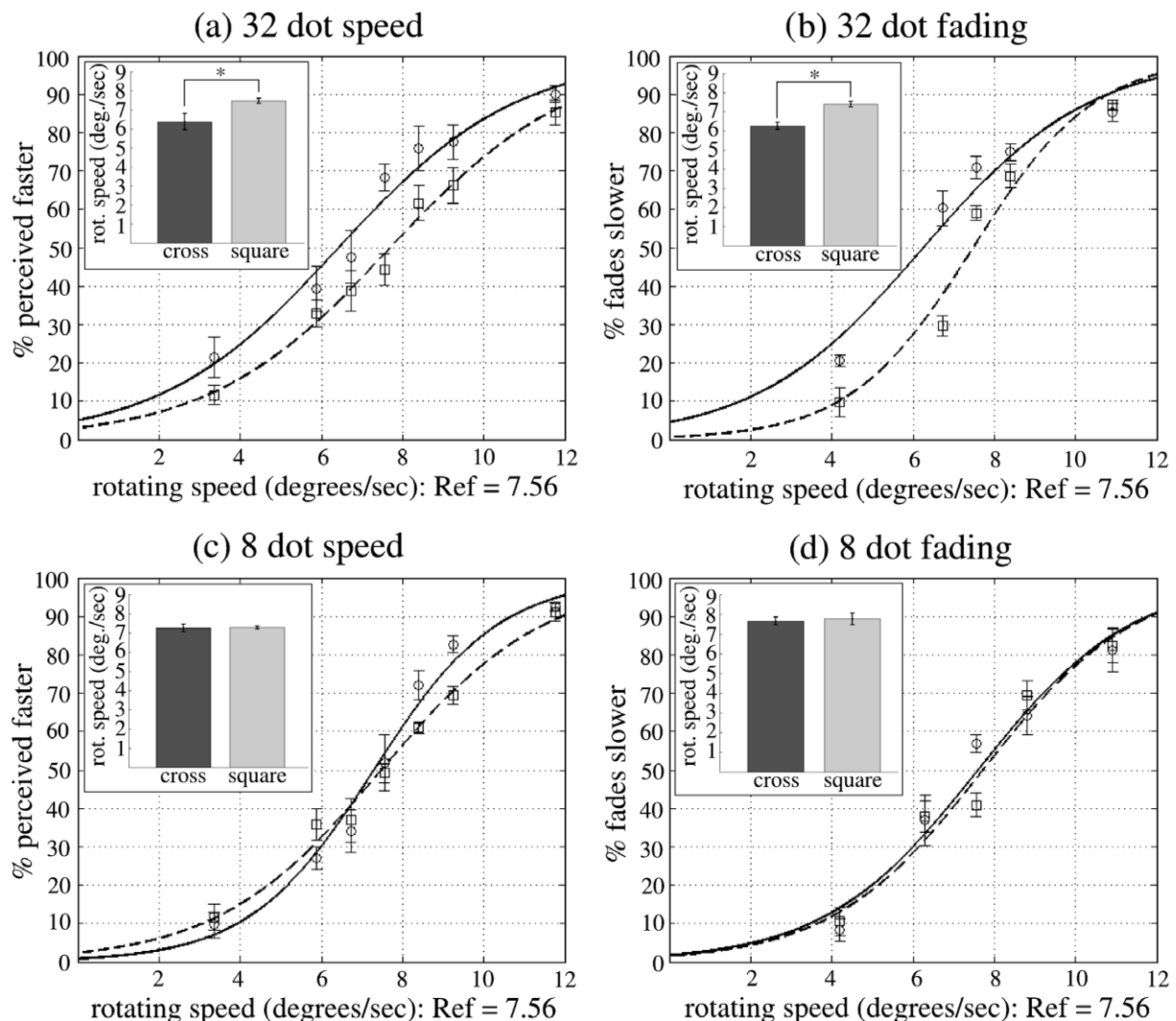


Fig. 4. The dotted cross appears to rotate faster and takes longer to undergo motion fading for the 32 dot, but not the 8 dot cases. (a) The results of Experiment 3.1a. (b) The results of Experiment 3.1b. (c) The results of Experiment 3.2a. (d) The results of Experiment 3.2b. The mean of the psychometric response functions across subjects is plotted on the four main graphs; solid lines with round datapoints represent trials where the test stimulus was a cross, dashed lines with square datapoints represent trials where the test stimulus was a square. The insets show the mean of the PSEs for the cross (dark grey) and square (light grey) test stimuli.

ing that the cross stimulus was perceived to rotate faster than the square stimulus. In Experiment 3.1b (Fig. 4b), the mean of the PSEs of the cross stimulus was also significantly smaller than the mean of the PSEs of the square stimulus [$t(7) = 2.829$, $p < 0.01$], meaning that motion fading occurred more slowly (i.e., took longer to fade) for the cross stimulus than for the square stimulus. A two-sample t -test permitted a direct comparison of the derived PSEs for the cross stimuli in the two experiments. This showed no significant difference between them [$t(14) = 0.054$, $p = 0.957$]. This indicates that if the angular velocity of the cross stimuli had been adjusted so it appeared to rotate at the same angular velocity as the fat ellipse, then motion fading would have occurred at the same time for the two configurations.

However, when the stimuli were defined by only 8 dots (Experiment 3.2), as shown in Fig. 3b, the cross stimulus was perceived to rotate as fast as the square stimulus [$t(5) = 0.091$, $p = 0.931$] (Fig. 4c), and motion faded equally fast for the two stimuli [$t(5) = 0.207$, $p = 0.844$] (Fig. 4d). A direct comparison of the two derived PSEs for the cross stimuli, using an independent samples t -test, showed no significant differences between them [$t(10) = 0.167$, $p = 0.871$].

5. General discussion

In motion fading, the motion component of the stimulus perceptually slows down, and ultimately stops. This is in contrast to the form component of the stimulus, which remains visible even after the motion has vanished. A recent paper (Hsieh & Tse, 2009a) has provided evidence that motion fading occurs because of adaptation among cortical neurons that are tuned to motion in the direction of the moving stimulus. When the angular velocity of stimulus motion is very low (i.e., near threshold for motion-tuned cells), adaptation results in the gradual loss of any motion signal in that direction, resulting, ultimately, in the perception of a stationary object when the object is in fact still moving.

The adaptation of motion sensitive neurons underlying motion fading makes it closely related to the motion after-effect (MAE). In the classic MAE, adaptation to a motion stimulus leads to illusory motion in the opposite direction being perceived over a subsequent stationary image (Wohlgemuth, 1911). Adaptation induces a shift in the population response to the stationary stimulus, causing the illusory perception of motion. Hsieh and Tse (2009a) concluded that motion fading and the MAE share a common process of neural adaptation in the same population of neurons. This is supported by two main findings: (a) the magnitude of both motion fading and MAE increase with eccentricity, (b) adaptation to a MAE-inducing stimulus decreases the TTS for a subsequently presented target undergoing motion fading (Hsieh & Tse, 2009a).

Compared to motion fading, the MAE has received a great deal of attention as a topic of empirical research and much is known about the phenomenon's neuronal bases. For example, it has been shown that the MAE is based on neural adaptation (i.e., modulation of gain control) near or at the input of MT (Kohn & Movshon, 2003). Van de Grind, van der Smagt, and Verstraten (2004; see also van de Grind, Lankheet, & Tao, 2003) showed how such adaptation might occur, on the basis of the gain-control model of Grunewald and Lankheet (1996). Moreover, Kohn and Movshon (2003) showed that the MAE mechanism is realized within the motion pathway and not the form pathway. This is consistent with the phenomenology of motion fading, where only the motion component appears to vanish from consciousness, while the form component remains visible. Because the data of Hsieh and Tse (2009a) imply that motion fading and the MAE occur because of adaptation in the same population of neurons, it follows that motion fading is

also realized in the motion pathway at or near the input to area MT.

It is well known that motion perception can be derived directly from the analysis of retinal motion by dedicated motion sensors in the cortex, or indirectly, by inferring motion from changes in the retinal position of objects, or their features, over time (Derrington, Allen, & Delicato, 2004). This latter process could be built upon motion signals derived from feature tracking (Del Viva & Morrone, 1998; Pack & Born, 2001; compare Lu & Sperling, 1995), which can overcome the ambiguity of motion signals arising from cells tuned to 'motion energy' (Adelson & Bergen, 1985; Ullman, 1979; Watson & Ahumada, 1985). We have previously shown that motion fading takes longer when there are virtual contours or endpoints that presumably emerge as a consequence of grouping procedures (Hsieh & Tse, 2007), even when individual dot motions are identical in a low-level sense among different dot configurations. We have also shown that perceived angular velocity can be affected by these form and grouping procedures (Hsieh & Tse, 2007, 2009a; Caplovitz & Tse, 2007; Kohler, Caplovitz, & Tse, 2009).

Here we have elaborated on these findings by showing that motion fading is driven by perceived angular velocity for both elliptical and other configurations, suggesting that the neural populations representing perceived motion, rather than those involved in detecting motion in the initial cortical input derived from the retinal image, underlie motion fading (and by extension also underlie the MAE). This perceived motion is not explicit in the retinal image; rather it is determined in part by grouping processes that construct distinct contours out of discrete elements in the image. It is the magnitude of emergent motion information associated with these constructed contours and not the local motion of the elements making up the contours that correlate most closely with motion fading, perceived angular velocity and perhaps conscious motion perception in general. While the stimulus-pairs used in this paper do not have identical local motions, this claim is supported by a previous set of studies (Hsieh & Tse, 2007) that varied configuration while keeping local dot motion magnitudes identical. Here, we have specifically demonstrated that it is not the mere presence of emergent motion signals that influences motion fading, but rather the magnitude of emergent motion signals that determines the time to perceived stopping. In order for motion fading to occur, the neural populations representing the emergent motion must fully adapt; presumably it takes longer for this to occur the faster the perceived angular velocity is, because represented motion magnitudes are larger, and therefore take longer to adapt to zero.

Generally, the results from the current study, together with our previous findings (Caplovitz & Tse, 2007; Hsieh & Tse, 2007, 2009a, 2009b; Kohler, Caplovitz, & Tse, 2009), support the conclusion that perceived angular velocity, and by extension motion fading, the MAE, and perhaps motion, as consciously perceived in general, are driven primarily by higher-level, constructed motion signals. These emergent motion signals, such as those derived from virtual contours or virtual trackable features, are constructed on the basis of, but are not identical to, low-level local motion information present in the image. Emergent motion signals emerge as a result of grouping and contour analysis procedures. Thus motion perception is inseparable from form analysis, because information derived from the form-processing of spatial configuration underlies the motion directions and magnitudes that are perceived as long as such grouping procedures can operate (for example, as long as the inter-dot distance is sufficiently small).

It is worth emphasizing that these higher-level motion signals do not necessarily exist in the image. There are cases where computed higher-order motion vectors (i.e. instantaneous motion magnitudes and directions perceived at a given location in the visual field) will align with motion vectors measurable in the image, but there are other cases where they will not align. Cases of non-

alignment make clear that motion vectors measurable in the image are used to compute higher-order motion vectors, but then appear to be discarded. This can lead to certain surprising paradoxes; For example, in the dotted stimuli used here, although the low-level dot motions are unambiguous with respect to the aperture problem, the angular velocity is misperceived despite the presence of local motion information that could in theory provide a more accurate percept. In particular, that the cross stimulus is perceived to rotate faster than the square (or the thin ellipse faster than the fat ellipse) reflects the primacy of the form-influenced emergent motion signals over locally detected ones, in deriving perceived motion (Caplovitz & Tse, 2007). In the case of the dotted stimuli used here and in our previous work, the different emergent contours (e.g. fat and thin ellipses, squares and crosses) in the grouped stimulus are only defined after a stage of global visual form analysis where the separate dots are grouped into contours and global shapes. The dots comprising these contours need not have more or less motion at the level of the image. The differences only arise in the emergent motion signals derived after a stage of grouping which presumably imbues them with the motion signals that they would have if they were real contours. It may be that the integration of these form and motion processes serves to resolve ambiguities that arise due to the small and simple receptive fields found early in the visual processing hierarchy (Adelson & Bergen, 1985; Fennema & Thompson, 1979; Marr, 1982; Nakayama & Silverman, 1988a, 1988b).

The present work adds to at least a decade of evidence that motion processing is influenced and constrained by form processing. Form analysis subserves motion processing in at least three important and related ways: (1) first, form processing permits figural segmentation dedicated to solving the problem of figure-to-figure matching over time that was revealed using transformational apparent motion as a probe (Caplovitz & Tse, 2006; Tse, 2006; Tse & Logothetis, 2002a; Caplovitz et al., 2006; Tse & Caplovitz, 2006); (2) second, form processing permits the definition of trackable features whose unambiguous motion signals can be generalized to ambiguously moving portions of an object to solve the aperture problem (Caplovitz & Tse, 2007b); (3) third, form processing permits the generation of emergent motion signals, for example, of virtual contours, that appear to underlie the conscious experience of motion (Caplovitz & Tse, 2007; Hsieh & Tse, 2007).

Because the form analyses that subserves motion processing are diverse in their functions, it is not surprising that they are realized in multiple cortical areas. The process of segmentation based on contour cues described under (1) above is primarily a ventral process involving the lateral occipital complex (LOC) and also retinotopic areas such as V2 and V4, and perhaps even V1 (Tse, 2006; Tse & Caplovitz, 2006). In contrast, the form analyses involved in specifying trackable features described in (2) above may primarily be a dorsal process involving V3A, with potential involvement of the LOC and hMT+ (Caplovitz & Tse, 2007; Tse & Caplovitz, 2006b). It is not yet clear where (3), the generation of virtual contours and their motion signals, arises, at least in the particular case examined here, of figures defined by moving dots.

fMRI studies that have examined how contours are integrated into global shapes reveal that contour integration activates V1 and V2 in humans and monkeys but produces strongest activation in the LOC (Altmann, Bühlhoff, & Kourtzi, 2003; Kourtzi, Erb, Grodd, & Bühlhoff, 2003ab). That striate cortex shows BOLD activation for a task that requires global contour integration is consistent with recent work in neurophysiology according to which V1 pyramidal cells with similar orientation preferences but non-overlapping receptive fields share long-range horizontal axonal connections (Gilbert and Wiesel, 1979, 1983, 1989; Li, Piëch, & Gilbert, 2008; Rockland, Lund, & Humphrey, 1982; Schmidt, Goebel, Lowel, & Singer, 1997; Stettler, Das, Bennett, & Gilbert, 2002). However, that

fMRI research implicates V1 in contour integration is perhaps surprising, given that, to date, V2 is the first area in the visual hierarchy where clearly emergent contours such as illusory contours have been shown to have a direct effect using single-unit recording (von der Heydt, Peterhans, & Baumgartner, 1984). While processing in V1 has traditionally (Hubel & Wiesel, 1968) been thought to be limited to the processing of local features, recent evidence has implicated early visual areas such as V1 and V2 in the processing of global shape (Allman, Miezin, & McCuiness, 1985; Gilbert, 1992, 1998; Tse, 2006; see also Fitzpatrick (2000); Lamme, Super and Spekreijse (1998) for reviews). In light of these findings, it is possible that emergent motion signals are in part generated as early as V1. Indeed, a simple, complex, or hypercomplex cell would presumably respond more to certain dot configurations than others, if the dots aligned with the orientation tuning of the cell, and the inter-dot distance were sufficiently close to assure that the dots fell within the cell's receptive field. However, these data cannot be used to establish, for example, that global processing takes place in V1. These data are also not sufficient to determine whether the activity seen in V1 arises because of bottom-up or top-down activation. The BOLD activity seen in V1 with contour integration processing is consistent with both possibilities and indeed may arise from both mechanisms.

The computation of virtual contours and contour discontinuities (such as corners, deep concavities, maxima of positive curvature, junctions, and terminators), plays a central role in all three types of form analysis, and by extension, in the specification of the motion signals to which these constructed form cues give rise. The analysis of form must proceed in parallel with the analysis of motion, in order to constrain the ongoing analysis of motion. Similarly, form processing is also informed by motion processing, as occurs in structure-from-motion.

In conclusion, local dot motion information is combined with information about the dot's spatial configuration to generate virtual contour motion signals when the dots are spaced sufficiently closely together. The motion signals associated with these virtual contours determine the angular velocity at which the contours appear to rotate. The time to stop in motion fading is not necessarily determined by the mere presence of an emergent contour, but rather by the magnitude of emergent motion signals. When the dots are closely spaced, individual dot motion signals appear to be discarded, or at least appear to play no role in motion fading. These results can be taken as further evidence for the inherently constructive nature of motion processing, and the importance of form operators in motion processing. In short, when virtual contour motion signals arise from moving dots, because of the closeness of their spacing, our perception of motion is driven by these emergent motion signals and not by the motion signals generated by the individual dots considered in isolation. In the case of motion fading, the time to stop is determined by perceived angular velocity derived from these virtual motion signals. Thus, motion fading is driven by perceived motion signals as opposed to the motion signals present in the stimulus.

References

- Adelson, E. H., & Bergen, J. R. (1985). Spatiotemporal energy models for the perception of motion. *Journal of the Optical Society of America A—Optics Image Science and Vision*, 2, 284–299.
- Adelson, E. H., & Movshon, J. A. (1982). Phenomenal coherence of moving visual patterns. *Nature*, 30, 523–525.
- Allman, J. M., Miezin, F., & McCuiness, E. (1985). Stimulus specific responses from beyond the classical receptive field: Neurophysiological mechanisms for local-global comparisons in visual neurons. *Annual Review of Neuroscience*, 8, 407–430.
- Altmann, C. F., Bühlhoff, H. H., & Kourtzi, Z. (2003). Perceptual organization of local elements into global shapes in the human visual cortex. *Current Biology*, 13(4), 342–349.

- Anstis, S. (2003). Moving objects appear to slow down at low contrasts. *Neural Networks*, 16, 933–938.
- Campbell, F. W., & Maffei, L. (1979). Stopped visual motion. *Nature*, 278, 192–193.
- Campbell, F. W., & Maffei, L. (1981). The influence of spatial frequency & contrast on the perception of moving patterns. *Vision Research*, 21, 713–721.
- Caplovitz, G. P., Hsieh, P.-J., & Tse, P. U. (2006). Mechanisms underlying the perceived angular velocity of a rigidly rotating object. *Vision Research*, 46(18), 2877–2893.
- Caplovitz, G. P., & Tse, P. U. (2006). The bar-cross-ellipse illusion: Alternating percepts of rigid and non-rigid motion based on contour ownership and trackable feature assignment. *Perception*, 35(7), 993–997.
- Caplovitz, G. P., & Tse, P. U. (2007). Rotating dotted ellipses: Motion perception is driven by grouped figural rather than local dot motion signals. *Vision Research*, 47(18), 1979–1991.
- Cohen, R. L. (1965). Adaptation effects and aftereffects of moving patterns viewed in the periphery of the visual field. *Scandinavian Journal of Psychology*, 6, 257–264.
- Del Viva, M. M., & Morrone, M. C. (1998). Motion analysis by feature tracking. *Vision Research*, 38, 3633–3653.
- Derrington, A. M., Allen, H. A., & Delicato, L. S. (2004). Visual mechanisms of motion analysis and motion perception. *Annual Review of Psychology*, 55, 181–205.
- Fennema, C., & Thompson, W. (1979). Velocity determination in scenes containing several moving objects. *Computer Graphics and Image Processing*, 9, 301–305.
- Fitzpatrick, D. (2000). Seeing beyond the receptive field in primary visual cortex. *Current Opinion in Neurobiology*, 10, 438–443.
- Gilbert, C. D. (1992). Horizontal integration and cortical dynamics. *Neuron*, 9, 1–13.
- Gilbert, C. D. (1998). Adult cortical dynamics. *Physiological Reviews*, 78, 467–485.
- Gilbert, C. D., & Wiesel, T. N. (1979). Morphology and intracortical projections of functionally characterised neurones in the cat visual cortex. *Nature*, 280, 120–125.
- Gilbert, C. D., & Wiesel, T. N. (1983). Clustered intrinsic connections in cat visual cortex. *Journal of Neuroscience*, 3, 1116–1133.
- Gilbert, C. D., & Wiesel, T. N. (1989). Columnar specificity of intrinsic horizontal and corticocortical connections in cat visual cortex. *Journal of Neuroscience*, 9, 2432–2442.
- Grunewald, A., & Lankheet, M. M. (1996). Orthogonal motion after-effect illusion predicted by a model of cortical motion processing. *Nature*, 384, 358–360.
- Hsieh, P.-J., & Tse, P. U. (2007). Grouping inhibits motion fading by giving rise to virtual trackable features. *Journal of Experimental Psychology: Human Perception and Performance*, 33, 57–63.
- Hsieh, P.-J., & Tse, P. U. (2009a). Motion fading and the motion after-effect share a common process of neural adaptation. *Attention, Perception and Psychophysics*, 71(4), 724–733.
- Hsieh, P.-J., & Tse, P. U. (2009b). Feature mixing rather than feature replacement during perceptual filling-in. *Vision Research*, 49, 439–450.
- Hubel, D. H., & Wiesel, T. N. (1968). Receptive fields and functional architecture of monkey striate cortex. *Journal of Physiology*, 195, 215–243.
- Hunzelmann, N., & Spillmann, L. (1984). Movement adaptation in the peripheral retina. *Vision Research*, 24, 1765–1769.
- Kohler, P. J., Caplovitz, G. P., & Tse, P. U. (2009). The whole moves less than the spin of its parts. *Attention, Perception and Psychophysics*, 71(4), 675–679.
- Kohn, A., & Movshon, J. A. (2003). Neuronal adaptation to visual motion in area MT of the macaque. *Neuron*, 39, 681–691.
- Kourtzi, Z., Erb, M., Grodd, W., & Bühlhoff, H. H. (2003a). Representation of the perceived 3-D object shape in the human lateral occipital complex. *Cerebral Cortex*, 13(9), 911–920.
- Lamme, V. A., Super, H., & Spekreijse, H. (1998). Feedforward, horizontal, and feedback processing in the visual cortex. *Current Opinion Neurobiology*, 8, 529–535.
- Li, W., Piëch, V., & Gilbert, C. D. (2008). Learning to link visual contours. *Neuron*, 57(3), 442–451.
- Lichtenstein, M. (1963). Spatio-temporal factors in cessation of smooth apparent motion. *Journal of the Optical Society of America*, 53, 304–306.
- Lu, Z., & Sperling, G. (1995). The functional architecture of human visual motion perception. *Vision Research*, 35, 2697–2722.
- MacKay, D. M. (1982). Anomalous perception of extrafoveal motion. *Perception*, 11, 359–360.
- Marr, D. (1982). *Vision*. New York: Freeman.
- Nakayama, K., & Silverman, G. H. (1988a). The aperture problem-I. Perception of nonrigidity and motion direction in translating sinusoidal lines. *Vision Research*, 28(6), 739–746.
- Nakayama, K., & Silverman, G. H. (1988b). The aperture problem-II. Spatial integration of velocity information along contours. *Vision Research*, 28(6), 747–753.
- Pack, C. C., & Born, R. T. (2001). Temporal dynamics of a neural solution to the aperture problem in visual area MT of macaque brain. *Nature*, 409, 1040–1042.
- Rockland, K. S., Lund, J. S., & Humphrey, A. L. (1982). Anatomical binding of intrinsic connections in striate cortex of tree shrews (*Tupaia glis*). *Journal of Comparative Neurology*, 209, 41–58.
- Schmidt, K. E., Goebel, R., Lowel, S., & Singer, W. (1997). The perceptual grouping criterion of colinearity is reflected by anisotropies of connections in the primary visual cortex. *European Journal of Neuroscience*, 9, 1083–1089.
- Stettler, D. D., Das, A., Bennett, J., & Gilbert, C. D. (2002). Lateral connectivity and contextual interactions in macaque primary visual cortex. *Neuron*, 36, 739–750.
- Stone, L. S., & Thompson, P. (1992). Human angular velocity perception is contrast dependent. *Vision Research*, 32, 1535–1549.
- Thompson, P. (1982). Perceived rate of movement depends on contrast. *Vision Research*, 22, 377–380.
- Thompson, P., & Stone, L. S. (1997). Contrast affects flicker and angular velocity perception differently. *Vision Research*, 37, 1255–1260.
- Thompson, P., Stone, L. S., & Swash, S. (1996). Angular velocity estimates from grating patches are not contrast-normalized. *Vision Research*, 36, 667–674.
- Tse, P. U. (2006). Neural correlates of transformational apparent motion. *NeuroImage*, 31(2), 766–773.
- Tse, P. U., Caplovitz, G. P. (2006). Contour discontinuities subserve two types of form analysis that underlie motion processing. In: *Progress in brain research: Visual perception part I, fundamentals of vision: Low and mid-level processes in perception* (Vol. 154, pp. 271–292). Elsevier.
- Tse, P. U., & Logothetis, N. K. (2002). The duration of 3-D form analysis in transformational apparent motion. *Perception and Psychophysics*, 64(2), 244–265.
- Ullman, S. (1979). *The interpretation of visual motion*. MIT Press: Cambridge, MA/London.
- van de Grind, W. A., Lankheet, M. J., & Tao, R. (2003). A gain-control model relating nulling results to the duration of dynamic motion aftereffects. *Vision Research*, 43, 117–133.
- van de Grind, W. A., van der Smagt, M. J., & Verstraten, F. A. (2004). Storage for free: A surprising property of a simple gain-control model of motion aftereffects. *Vision Research*, 44, 2269–2284.
- von der Heydt, R., Peterhans, E., & Baumgartner, G. (1984). Illusory contours and cortical neuron responses. *Science*, 224(4654), 1260–1262.
- Watson, A. B., & Ahumada, A. J. Jr. (1985). Model of human visual-motion sensing. *Journal of the Optical Society of America A-Optics Image Science and Vision*, 2, 322–341.
- Wohlgemuth, A. (1911). On the after-effect of seen movement. *British Journal of Psychology*. PhD thesis, University of London. Cambridge University Press.